Nuclear Instruments and Methods in Physics Research B 267 (2009) 3245–3248

Contents lists available at ScienceDirect

Nuclear Instruments and Methods in Physics Research B

journal homepage: www.elsevier.com/locate/nimb

Growth of silicon nitride films by bombarding amorphous silicon with N^+ ions: MD simulation

F. Gou [a], M.A. Gleeson [a], A.W. Kleyn [a], R.W.E. van de Kruijs [a], A.E. Yakshin [a], F. Bijkerk [a,b,*]

[a] FOM-Institute for Plasma Physics Rijnhuizen, Ass. EURATOM-FOM, Nieuwegein, P.O. Box 1207, 3430 BE Nieuwegein, The Netherlands
[b] MESA+Institute for Nanotechnology, University Twente, Enschede, The Netherlands

ARTICLE INFO

Article history:
Available online 18 June 2009

PACS:
31.15.xv
61.72.uf
68.55.Ln
81.15.-z

Keywords:
Molecular dynamics calculations in atomic and molecular physics
Silicon, doping and ion implantation
Ion implantation thin films
Deposition films and coatings

ABSTRACT

In this study, the molecular dynamics simulation method was employed to investigate the growth of silicon nitride films by using N^+ ions, with energies of 50, 100, 150 and 200 eV, to bombard an amorphous silicon surface at 300 K. After an initial period of N^+ bombardment, saturation of the number of N atoms deposited on the surface is observed, which is in agreement with experiments. During subsequent steady state deposition, a balance between uptake of N by the surface and sputtering of previously deposited N is established. The $Si(N_x)$ (x = 1–4) and $N(Si_y)$ (y = 1–3) bond configurations in the grown films are analyzed.

1. Introduction

Silicon nitride films have been widely used as passivation layers and diffusion barriers in multilayer devices [1–5]. Low energy reactive ion deposition methods have been employed to fabricate these films [6–8]. In order to improve the performance of silicon-nitride-based devices and to get insight into the growth mechanisms of these films, experimental research has been conducted on N^+ and N_2^+ interacting with silicon [6,8–10]. However, fundamental understanding of the basic mechanisms (the formation of silicon nitride, kinetics of film growth under energetic ion bombardment, etc.) of the interaction process is still incomplete.

Molecular dynamics method (MD) is a powerful tool for investigating dynamic processes at the atomic scale. This method has been widely used to study ions interacting with surfaces [11–13]. Many MD simulations on bulk amorphous silicon nitride have been performed [14–15]. However, little work has been done on simulating the growth of amorphous silicon nitride films [16]. The aim of this work is to understand the dynamics of N^+ interacting with silicon and subsequent film growth at the atom-scale level. This study will be useful for understanding the silicon nitride film growth mechanisms present in the experiment.

2. Computational details

In order to simulate N^+ interacting with silicon surfaces, we employed a classical molecular dynamics method with empirical bond order potentials. The simulation method has been described in detail in previous publications [17,18]. In the current simulations, the Tersoff-type potential was chosen to describe interactions in the Si–N system [19,20]. Note that in the simulation of N–N interactions only the repulsive term is used. This assumption is employed in many MD simulations of amorphous silicon nitride [15,20]. In addition, it is assumed that ions are neutralized within a distance of a few Å from the surface [21]. Therefore, in current simulations, N^+ ions at the surface are regarded as neutral atoms. All simulations were carried out with LAMMPS (Large-scale Atomic/Molecular Massively Parallel Simulator) [22].

In the current simulations, the initial bulk amorphous silicon was prepared by depositing 10 eV Si atoms on a Si(1 0 0) 2×1 surface with dimensions of $21.74 \times 21.74 \times 32.61$ Å at 300 K. The initial substrate cell consisted of 768 Si atoms. During deposition, the two bottom layers, containing 64 Si atoms, were fixed. After

* Corresponding author. Address. FOM-Institute for Plasma Physics Rijnhuizen, Ass. EURATOM-FOM, Nieuwegein, P.O. Box 1207, 3430 BE Nieuwegein, The Netherlands. Tel.: +31 30 6096837; fax: +31 30 6031204.
E-mail address: F.Bijkerk@rijnhuizen.nl (F. Bijkerk).

0168-583X/$ - see front matter © 2009 Elsevier B.V. All rights reserved.
doi:10.1016/j.nimb.2009.06.091

deposition the entire cell was relaxed for 10 ps at 300 K. The relaxed sample consisting of 2885 Si atoms in a $21.74 \times 21.74 \times 123.76$ Å cell is used as the starting configuration for the current MD simulations. During N^+ bombardment, the 768 Si atoms belonging to the initial substrate were fixed to anchor the simulation cell and to simulate a bulk substrate. In all simulations, the simulation cell has periodic boundaries in the *x*- and *y*-directions. The incident energies of N^+ used are 50, 100, 150 and 200 eV and the incident angle is normal to the surface. The surface temperature is 300 K.

3. Results

The number of N atoms deposited on the surface at 300 K as a function of the number of incident N ions for 50, 100 150 and 200 eV incident energies is presented in Fig. 1. From this figure, it is noted that during the initial stages the deposition of N on the surface is not sensitive to the incident energy and most incident ions remain on the surface. After the initial sharp increase in the number of deposited N atoms on the surface, saturation is observed. In steady state, the total number of N atoms deposited for a given exposure increases with increasing incident energy. The increase in the number of deposited N atoms from 50 to 100 eV is less than that from 100 to 200 eV. Saturation of N atom deposition at different energies has been experimentally observed by Park et al. [7]. They observed a saturation of N atoms at a concentration of $\sim 20.0 \times 10^{14}$ atoms/cm^2 on the surface after exposure to $\sim 8.0 \times 10^{15}$ ions/cm^2 N_2^+ at 100 eV. In current simulations it is found that when the uptake of N atoms reaches saturation, the concentration on the surface is equivalent to approximately 43.3×10^{14} atoms/cm^2 for a 50 eV N^+ ion dose of 1.75×10^{16} ions/cm^2, which corresponds to 8.77×10^{15} ions/cm^2 for 100 eV N_2^+. The good agreement with the experimental data shows that MD simulations can reliably predict the ion dose that results in saturation. At saturation, the simulated N atom concentration is two times greater than that reported experimentally. However, the difference is still within the quoted experimental error.

Park et al. proposed that the saturation behavior of N on the modified surface is caused by the concerted effects of penetration, self-sputtering and scattering of incident N^+ ions [7]. They defined self-sputtering as the sputtering of previously deposited N atoms by subsequent incident N_2^+ ions. We also adopt this definition and in order to characterize the balance between sputtering, deposition and scattering, Fig. 2 shows the cumulative number of incident N^+ ions along with the resultant instances of self-sputtering, deposition and scattering during the bombardment as a function of the number of incident N^+ ions at 100 eV. During the initial stages (film growth period), most incident N^+ ions deposit on the substrate. Only a few atoms are removed from the growing film via scattering or self-sputtering. During this period, the number of N atoms removed from the surface via scattering is similar to that via self-sputtering. However, upon N saturation in the grown film, the number of N atoms removed by self-sputtering is significantly enhanced. Note in the figure that only a few incident N^+ ions scatter away from the surface after saturation. At this point, the film growth has reached a steady state resulting essentially from a balance between deposition and sputtering.

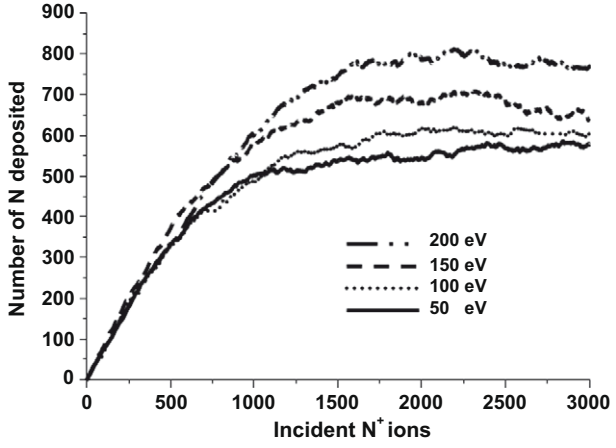

Fig. 1. Number of N atoms accumulated on the surface at 300 K as a function of the number of incident N^+ ions for ion energies of 50, 100 150 and 200 eV.

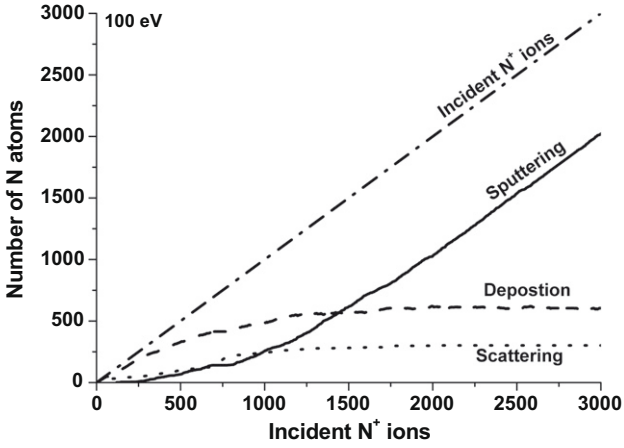

Fig. 2. Cumulative number of incident N^+ ions, self-sputtering, deposition and scattering events during bombardment as a function of the number of incident N^+ ions for 100 eV at 300 K. The number of incident N^+ ions is equal to the sum of self-sputtering, scattering and deposition.

When N^+ ions bombard the Si surface, some Si–Si bonds are broken and Si–N bonds are formed. A Si atom can bind with 4 N atoms while N can combine with three Si atoms to form the ideal Si_3N_4 stoichiometry. In order to characterize the chemical composition of the grown films, four Si–N_x (x = 1–4) bond configurations are defined. Hereafter, they are referred to as Si(N_x). These four bond configurations can be experimentally determined [8]. Similarly, three N–Si_y (y = 1–3) bond configurations are defined, denoted by N(Si_y). In the simulations we can observe the presence of one or two N dangling bonds for N(Si_y) (y = 1–2) bond configurations, since the formation of N–N bonds is prohibited in the current model. In contrast, relatively few Si dangling bonds are predicted by the simulations. Hence the bond order of Si(N_x) (x = 1–3) species can be considered as being fully satisfied by $(4 - x)$ additional Si–Si bonds.

Table 1 shows the saturation densities of Si(N_x) and N(Si_y) as a function of the incident energy after exposure to 3000 N^+. Note that the density of the bond configuration is defined as the number of bond per Å^3. For all incident energies we observe that Si(N_4) is dominant among the Si(N_x) components. Higher energies result in a higher Si(N_4) bond density. For the N(Si_y) components shown in Table 1, it is noted that the contents of N(Si_2) and N(Si_3) in the

Table 1
The densities of Si(N_x) (x = 1–4) and N(Si_y) (y = 1–3) in the nitride layer obtained at different incident energies after exposure to 3000 N^+. Here, Si(N_x) and N(Si_y) represent the Si–N(x) and N–Si(y) bond configurations.

Ei (eV)	Bond density (Å^{-3})						
	Si(N_1)	Si(N_2)	Si(N_3)	Si(N_4)	N(Si_1)	N(Si_2)	N(Si_3)
50	0.0873	0.0499	0.0499	0.3134	0.0671	0.4849	0.3288
100	0.1247	0.0593	0.0717	0.3087	0.1154	0.5784	0.2619
150	0.1044	0.0904	0.0655	0.3414	0.1232	0.6470	0.2806
200	0.1092	0.0764	0.0842	0.4147	0.1107	0.6580	0.4272

film increase with increasing incident energy. $N(Si_2)$ is the most abundant in all four films. Hence, the simulation predicts an N-rich nitride layer formation.

Figs. 3(a) and (b) show the evolution of densities of $Si(N_x)$ and $N(Si_y)$ for 50 eV N^+ bombardment. During the initial stage, with increasing exposure to N^+, the densities of $Si(N_1)$, $Si(N_2)$ and $Si(N_3)$ increase, reach an maximum and then decreases; while the density of $Si(N_4)$ continuously increases. Before the densities of $Si(N_x)$ ($x = 1–3$) reach maximum, $Si(N_1)$ is dominant, followed by $Si(N_2)$, $Si(N_3)$ and $Si(N_4)$. Once N saturates in the film, the densities of $Si(N_x)$ remain effectively constant. At the saturation, the $Si(N_4)$ component is dominant and the densities of $Si(N_1)$, $Si(N_2)$ and $Si(N_3)$ components are all at a low level. For $N(Si_y)$ shown in Fig. 3(b), note that with increasing N^+ exposure, $N(Si_2)$ and $N(Si_3)$ increase. Prior to N saturation, the $N(Si_3)$ component is dominant. However, after N saturation, the $N(Si_3)$ component decreases slightly, while the density of $N(Si_2)$ steadily increases. The density of $N(Si_2)$ increases in a relatively gradual fashion for most of the exposure period. Only at the very end does this functional group appear to saturate. This behavior results in a density of $N(Si_3)$ that is less than that of $N(Si_2)$.

Figs. 4(a) and (b) show the corresponding evolution of $Si(N_x)$ and $N(Si_y)$ densities for 150 eV N^+ bombardment. With increasing N^+ dose, the density of $Si(N_4)$ in the growing film increases in a more gradual fashion than that observed for 50 eV bombardment due in part to sputtering of Si. Similar to the behavior at 50 eV, the densities of $Si(N_1)$ and $Si(N_2)$ in the films decrease after reaching an maximum. Note that unlike at 50 eV (when the maximum of the three species occurs at roughly similar exposure), the maximum intensities occur in a clear sequential fashion: $Si(N_1) \rightarrow Si(N_2) \rightarrow Si(N_3)$. With N saturation in the film, the density of $Si(N_4)$ reaches a steady state, while the densities of $Si(N_x)$ ($x = 1–3$) continue to decrease gradually and reach steady state only at the end of the simulation. For $N(Si_y)$, shown in Fig. 4(b), it is found that the density of $N(Si_2)$ becomes larger than that of $N(Si_3)$ very quickly after the initial exposure and subsequently become the dominant $N(Si_y)$ component in the layer. The content of $N(Si_2)$ continuously increases for most of the N exposure period. For $N(Si_3)$, only during the initial stages is its content larger than that of $N(Si_2)$.

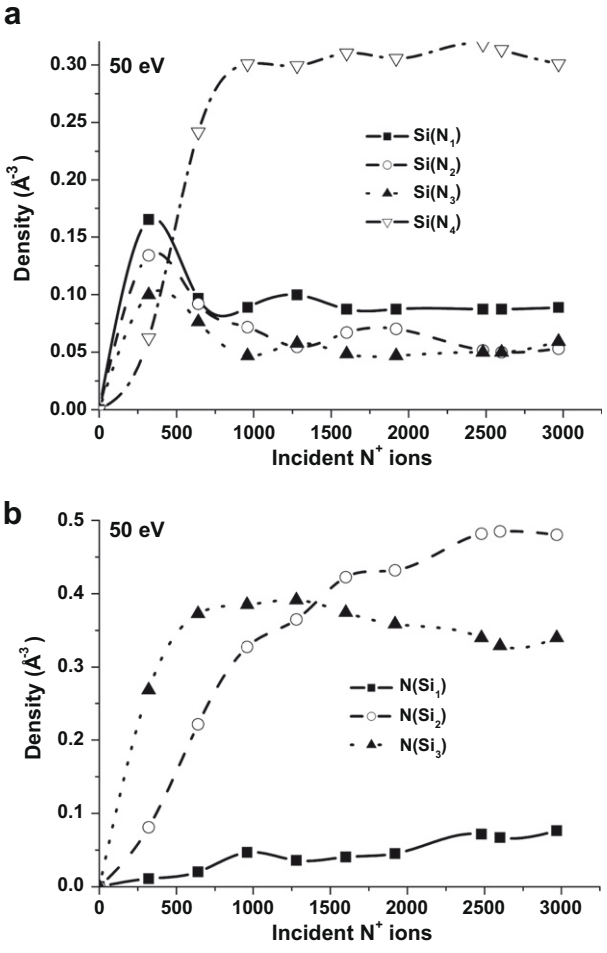

Fig. 3. Evolution of densities of (a) $Si(N_x)$ ($x = 1–4$) and (b) $N(Si_y)$ ($y = 1–3$) during exposure to 50 eV N^+ ions.

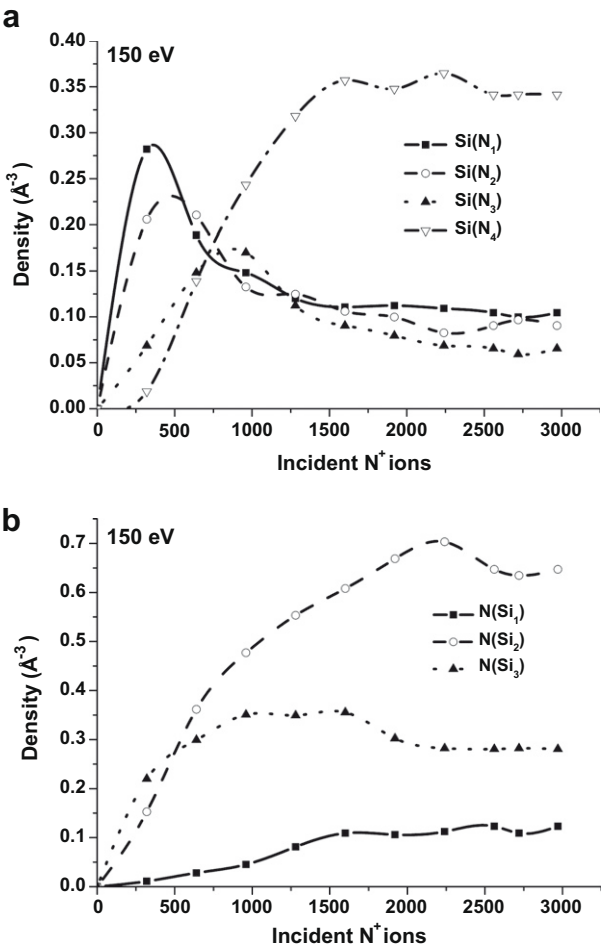

Fig. 4. Evolution of densities of (a) $Si(N_x)$ ($x = 1–4$) and (b) $N(Si_y)$ ($y = 1–3$) during exposure to 150 eV N^+ ions.

The results of $Si(N_x)$ in the films (shown in Figs. 3(a) and 4(a)) are consistent with experimental results obtained by Kusunoki et al. [8]. In their experiments, silicon nitride films were produced by 100–1000 eV N_2^+ ion bombardment of a Si(1 0 0) (which can be regarded as equivalent to exposure to 50–500 eV N^+ ions). The populations of $Si(N_x)$ bond configurations obtained from Si2p XPS spectra were analyzed by curve fitting. They found that at energies less than 1000 eV the densities of $Si(N_1)$ increase in the initial stage, then decrease with increasing ion dose and finally reaching a steady value at saturation, while the $Si(N_4)$ component continuously increases before reaching a steady state. At saturation the $Si(N_4)$ component is dominant. This behavior is indeed predicted by the MD simulations shown in Figs. 3 and 4. At low energies, especially for 50 eV the MD method can quantitatively reproduce

the relative densities of $Si(N_x)$ (x = 1–4) obtained from those experiments. However, when the incident energies of N^+ are higher than 100 eV, the quantitative agreement between simulation and experiment deteriorates. In the experiments it is found that at saturation the densities of the $Si(N_x)$ (x = 1–4) components for 300 eV N_2^+ ions were almost same, whereas in our simulations the $Si(N_4)$ component is clearly dominant.

The difference between simulations and experiments at higher energies may be attributable to two factors. First, in order to compare to the experimental data using N_2^+ bombardment, it is assumed that when N_2^+ is neutralized and dissociates, the kinetic energy is distributed equally over two N atoms. However, scattering calculations demonstrate that the kinetic energy of neutral N_2 is not necessarily equally distributed [17]. Second, in our chosen model no attractive term is included to describe the N–N interactions. This assumption prohibits two N atoms from forming N_2 during collisions, although N_2 formation is experimentally observed [7].

Based on the data shown in Table 1, the calculations demonstrate that an N-rich nitride layer with an atomic ratio of $N/Si_{reacted}$ greater than 1.6 is formed, which is significantly higher than the ideal stoichiometric ratio of 0.75. This suggests that at saturation a N-rich layers can be formed. This may still be due to the deficiencies inherent in not considering the attractive term during N–N interactions. In order to probe the effects of an N–N attractive term on the simulation results, some test simulations were performed at 100 eV. After saturation occurred, the original attractive term of N–N was reintroduced. As a result, it was found that N atoms in the deposited film (produced while excluding the attractive term) formed N_2 and desorbed Use of the "correct" N–N attractive potential invariably results in the desorption of all nitrogen from the surface in the form of N_2. Other test runs, using a reduced N–N attractive term, also showed a significant decrease in the ratio of $N/Si_{reacted}$. Both tests clearly indicate that neglecting the attractive term leads to a too high surface N-atom concentration, whereas including it results in excessive N removal. In order to improve the current modeling, a new potential containing an N–N attractive term suitable for film growth is necessary.

4. Conclusion

Molecular dynamics simulations were performed to study the nitridation of silicon by low energy N^+. The simulation results show

(1) the uptake of N in films depends on the incident energies;
(2) self-sputtering, scattering and penetration lead to saturation of N in the films;
(3) in all films the N atoms react with Si to form Si–N bonds. Si atoms are fully saturated by N or Si, while N atoms are not completely saturated and some dangling bonds are present.

Acknowledgements

This work is part of the EURATOM/FOM Industrial Partnership Programme I10 ('XMO') which is carried out under contract with Carl Zeiss SMT AG, Oberkochen and the 'Stichting voor Fundamenteel Onderzoek der Materie (FOM)', the latter being financially supported by the 'Nederlandse Organisatie voor Wetenschappelijk Onderzoek (NWO)' and SenterNovem through the EAGLE/ACHieVE project carried out in collaboration with ASML and Carl Zeiss SMT AG.

References

[1] T.N. Chen, D.S. Wuu, C.C. Wu, C.C. Chiang, H.B. Lin, Y.P. Chen, R.H. Horng, Thin Solid Films 514 (2006) 188.
[2] M. Kunst, O. Abdallah, F. Wünsch, Sol. Energy Mater. Sol. Cell. 72 (2002) 335.
[3] F.E. Fernández, E. Rodrígez, M. Pumarol, T. Guzmán, W. Jia, A. Martínez, Thin Solid Films 377–378 (2000) 781.
[4] M.M.J.W. van Herpen, R.W.E. van de Kruijs, D.J.W. Klunder, E. Louis, A.E. Yakshin, S.A. van der Westen, F. Bijkerk, V. Banine, Opt. Lett. 33 (2008) 560.
[5] R.W.E. van de Kruijs, M.M.J.W. van Herpen, E. Zoethout, E. Louis, A.E. Yakshin, D.J.W. Klunder, S. Mullender, V. Banine, F. Bijkerk, J. Appl. Phys., in preparation.
[6] D.H. Baek, H. Kang, J.W. Chung, Phys. Rev. B 49 (1994) 2651.
[7] K.H. Park, B.C. Kim, H. Kang, J. Chem. Phys. 97 (1992) 2742.
[8] I. Kusunoki, T. Takaoka, Y. Igari, K. Ohtsuka, J. Chem. Phys. 101 (1994) 8238.
[9] B.C. Kim, H. Kang, C.Y. Kim, J.W. Chung, Surf. Sci. 301 (1994) 295.
[10] J.S. Pan, A.T.S. Wee, C.H.A. Huan, H.S. Tan, K.L. Tan, Vacuum 47 (1996) 1495.
[11] D.-H. Kim, G.-H. Lee, S. Yup Lee, D. Hyun Kim, J. Cryst. Growth 286 (2006) 71.
[12] M.E. Bachlechner, R.K. Kalia, A. Nakano, A. Omeltchenko, P. Vashishta, I. Ebbsjö, A. Madhukar, G.-L. Zhao, J. Eur. Ceram. Soc. 19 (1999) 2265.
[13] F. Gou, A.W. Kleyn, M.A. Gleeson, Int. Rev. Phys. Chem. 27 (2008) 229.
[14] N. Umesaki, N. Hirosaki, K. Hirao, J. Non-Cryst. Solids 150 (1992) 120.
[15] F.D. Mota, J.F. Justo, A. Fazzio, J. Appl. Phys. 86 (1999) 1843.
[16] X.-Y. Guo, P. Brault, Surf. Sci. 488 (2001) 133.
[17] F. Gou, M.A. Gleeson, A.W. Kleyn, Phys. Chem. Chem. Phys. 8 (2006) 5522.
[18] F. Gou, M.A. Gleeson, J. Villette, A.W. Kleyn, Nucl. Instr. and Meth. B 247 (2006) 244.
[19] J. Tersoff, Phys. Rev. B 38 (1988) 9902.
[20] F. de Brito Mota, J.F. Justo, A. Fazzio, Phys. Rev. B 58 (1998) 8323.
[21] H.D. Hagstrum, Electron and Ion Spectroscopy of Solids, Plenum, New York, 1978. p. 1988.
[22] S. Plimpton, J. Comput. Phys. 117 (1995) 1.